Mapping of plasticity and stress-related markers in acute and chronic stress in rats

Master in Neuroscience, thesis. Achucarro Basque Center for Neuroscience. UPV/EHU.

Student: Nagore Torres Durán
Codirector 1: Alejandro Carretero Guillén
Codirector 2: Elena Alberdi Alfonso

Leioa, 15th June 2022

ABSTRACT

Stress is a physiological response to any kind of demand or threat that challenges the homeostasis of the organism. Although stress increases alertness and performance, excessive stress often negatively affects cognitive processes such as learning. The present work aims to help elucidating the molecular mechanism underlying the effects of acute and chronic stress on associative learning in rats. Immunohistochemical analysis centred on synaptic plasticity and synapse inhibition were carried out. Indeed, parvalbumin (PV) and calretinin (CR) interneurons were labelled to quantify PV+ and CR+ cells and protein expression. The expression of N-methyl-D-aspartate receptor (NMDAR), relevant in long-term potentiation, was also assessed within those cells. Confocal image analysis was accomplished combining Fiji-ImageJ and Pythons software, a method developed in our lab. This work shows stress-induced alterations in PV and CR expression, but not in NMDAR1. These results add to the increasingly growing field of GABAergic signalling dysfunction in stress-related illnesses that hopefully will provide clinical applications in the future.

INTRODUCTION

Stress is an innate response to an overload of stimuli or an overwhelming situation that impairs the homeostasis of the organism. Although this physiological phenomenon is fundamental to survival, it is also strongly related to several brain disorders including depression, anxiety and post-traumatic stress disorder (Hariri and Holmes, 2015; Godoy et al., 2018). Higher animals, in particular, have evolved elaborate physiological and neurobiological systems to notice, react, and adapt to all kind of stressors. As any external stimulus, stressors are perceived by sensory input. When that information reaches to the brain nuclei, a stress-response is triggered adapted to the nature of the stimulus. Since a great diversity of stressors exist, the organism has developed a wide variety of neurobiological responses.

Classically, the systems activated in stress are divided into two, depending on the time they take for an actionable output, although a combination of both is what commonly occurs, interplaying cooperatively and even synergistically (Akirav and Richter-Levin, 2002). For example, acute stressors require fast and immediate responses, which is mainly achieved, at least in a first phase, by the so-called sympathetic-adreno-medullar (SAM) axis. Preganglionic sympathetic neurons project to the adrenal medulla in the adrenal gland, causing catecholamines (adrenaline and noradrenaline) to be released to the circulation. Not only adrenaline and noradrenaline but also other monoamines, including dopamine and serotonin, contribute to the stress response. Because monoamines generally act through G protein-coupled receptors, which rapidly activate downstream effectors, the rapid rise in their level is quickly translated into altered functioning of neurons that express these receptors (Jöels and Baram, 2009).

Following the fast changes evoked by the SAM axis, the second major system comes into play: the hypothalamic-pituitary-adrenal (HPA) axis. The effects of HPA are considered slower but resulting in amplified long-lasting responses typical of chronic stress (Joëls and Baram, 2009; Godoy et al., 2018). This pathway is, in part, activated trough the action of the catecholamines released in consequence of acute stress, activating paraventricular nucleus of the hypothalamus (Calogero et al., 1988). A cascade of hormonal communication between the structures of the axis takes places next. In short, the paraventricular nucleus secrets corticotropin-releasing hormone (CRH) which acts on the pituitary gland, and the later then secrets the adrenocorticotropic hormone (ACTH) that travels to the adrenal cortex of the

adrenal gland, mediating the release of glucocorticoids. Glucocorticoids interact with mineralocorticoid and glucocorticoid intracellular receptors which are transcription factors, leading to changes in gene expression (Sharpley, 2009).

Centring on actions taken on the brain, monoamines and glucocorticoids exert their effects in a site-specific way. To that end, the site of release coupled with receptor localization provides a fine-resolution spatial specificity regarding the actions of both stress mediators. Consequently, there are brain regions involved in different aspects of the stress response. For instance, the basolateral amygdala, which is affected by noradrenaline, dopamine, CRH and corticosteroids, is responsible for promoting the state of alertness and vigilance. Also the basolateral amygdala, together with the prefrontal cortex and hippocampus, processes emotional and contextual aspects of stress (Jöels and Baram, 2009).

As can be seen, many brain regions are affected by stress, thus, any other process regulated by those areas will possibly be affected. Indeed, in a project led by our collaborators to study the influence of stress in learning, rats subjected to acute stress performed worse than not-stressed control group. The associative learning of animals was assessed trough the operant conditioning chamber test (the Skinner box), on which stressed rats showed a delayed achievement, because of their impaired learning skills. Concomitantly measured electrophysiological recordings in different brain areas demonstrated changes in power spectra of local field potentials (LFPs), which may be indicative of the stress state of the animals (unpublished data).

To understand how learning is affected under stress at a deeper level, molecular events involved in these processes should be explored. Long-term synaptic plasticity refers to a long-lasting experience-dependent change in the efficacy of synaptic transmission that involve strengthening or weakening the synapse, processes named long-term potentiation (LTP) and depression (LTP), respectively. One of the pathways for LTP is dependent on the N-methyl-D-aspartate receptor (NMDAR) in glutamatergic synapses. NMDAR together with alpha-amino-3-hydroxy-methyl-4-isoxazole propionic acid receptor (AMPAR) act to trigger action potentials. Both receptors are ionotropic and require binding of glutamate neurotransmitter to be activated. The main difference between the two is that at negative membrane potentials close to resting values, magnesium ions enter the pore of NMDAR, blocking the passage for all other ions. Therefore, when glutamate is released to the synaptic cleft and binds its receptors, AMPAR will be opened allowing a strong influx of sodium ions to enter the cell. This sets the conditions for NMDAR activation, because upon depolarization the magnesium is expelled from the pore, allowing cations to pass and contributing to the membrane depolarization. The bigger the amount of activated AMPAR and NMDAR in the postsynaptic membrane, the higher is the depolarization and, in turn, there is a greater chance for an action potential to be fired. In conclusion, this mode of LTP makes synapses more excitable (Lüscher and Malenka, 2012).

Currently, an increasingly adopted perspective to study the biochemistry of stress in the brain is to focus on the GABAergic system, crediting the role of interneurons on shaping the structure and physiology of the brain (Albretch et al, 2021). Alterations in GABAergic signalling are considered to be very relevant in inhibition/excitation balance. Among the interneuron subtypes, those expressing calcium binding proteins such as calretinin (CR) and parvalbumin (PV) are ones of the most studied. The role of these molecules is to buffer intracellular calcium concentrations in neurons and thereby modulate calcium transients in activated neurons (Schwaller, 2012). Alteration in these markers, in particular parvalbumin, can lead to brain network dysfunction (Nobili et al., 2018).

HYPOTHESIS AND OBJECTIVES

In line with the commented above, the present work aims to provide some clarity to GABAergic signalling in the scope of acute and chronic stress, as well as its impact on learning-related molecular mechanisms. More specifically, PV and CR interneuron subtypes sensitive to stress will be mapped trough immunohistochemistry. For the study of acute stress, the rats used in our collaborator's experiments will be used, on which stress was induced by electric footshocks. As impairment in associative learning of these animals may be reflected in altered NMDAR expression, this receptor will also be labelled with immunohistochemistry. For the chronic stress, organotypic hippocampal slices treated with dexamethasone, a strong synthetic glucocorticoid, will be the subject of study. The hippocampal slices will also be stained for all three PV, CR and NMDAR markers.

Along with the stated objectives, and additional and equally important pursuit is to develop an objective method to analyze the obtained data. For that, a computer-assisted image analysis will be elaborated, which will provide automation, traceability and reproducibility. Apart from working efficiently and saving time, a desirable advantage of software is that helps gaining deeper insights into the data that could have missed otherwise, exploiting to the fullest the worthy information within it.

In accordance of what so far have been laid out, we expect to find significant alterations in stress condition in plasticity- and stress-related markers (PV, CR, NMDAR), both in acute stress rat model and chronically stressed organotypic hippocampal slices.

MATERIALS AND METHODS

Animals and experimental background

Brains of male Wistar rats (3 months old, 250-300 g) fixed by perfusion with 4 % paraformaldehyde were assigned to this project. In total, 10 brains of stressed rats and 9 brains of not-stressed control rats were used. The animals had previously undergone the Skinner box test, an operant conditioning test, led by our collaborators to evaluate the learning performance when stressed. The Skinner box was equipped with levers and feeders. Feeders delivered a small pellet after each lever press. Conditioning took place during 10 successive sessions (1 session/day), in which animals were allowed to press the lever to receive pellets from the feeder using a fixed-ration (1:1) schedule. Stressed rats presented a slower learning curve comparing to controls, nevertheless, both groups achieved same performance-level by the las conditioning sessions.

Electrophysiological activity was registered meanwhile with electrodes placed in different areas of the brain. Precisely, in cortical and subcortical structures traditionally considered crucial for learning (the prelimbic cortex, PrL, and nucleus accumbens, NaC), and stressful situations (the basolateral amygdala, BLA) and rewarding (NaC). They found changes in power spectra of LFPs in all areas, which may be indicative of the stress state of the animals. Acute stress was induced by an electric footshock (see Berardi et al., 2014) 7 days right before the training in the Skinner box and a second electric footshock 24 h before being sacrificed, while the control group did not receive neither of the electric footshocks. These two electric footshocks consolidate the acute stress model addressed on this work. Animals were sacrificed soon after the last electric footshock.

Brain tissue preparation and immunohistochemistry

The brains were cut into 50 μm-thick serial coronal sections using a Leica VT1200 S vibratome. Brains were previously embedded in 4 % agar blocks to preserve tissue

consistency while cutting. The vibration amplitude of the blade was 1.35 mm with a 1.5 mm/s speed of forward advance. Sections were collected in series and stored in PBS (pH 7.4) with 0.2% sodium azide at 4 ºC until staining. Immunohistochemistry was carried out to label PV and CR interneuron markers and NMDAR1 (a subunit of NMDAR) involved in LTP. Free-floating sections were first washed in PBS. Non-specific binding was prevented by incubating the sections for 1 h 30 mins in PBS containing 5 % goat normal serum (GNS) and 3 % bovine serum albumin (BSA) and 0.5 % Triton X-100. Subsequently, the sections were incubated overnight at 4 ºC with various primary antibodies. Precisely, the following primary antibodies were used: rabbit anti-PV (1:1000 dilution; Invitrogen, PA1-933), guinea pig anti-CR (1:500 dilution; Synaptic Systems, 214 104) and mouse anti-NMDAR1 (1:500 dilution; Merk Millipore, MAB363). After six 10 min-washes with PBS, the sections were incubated with corresponding fluorophore-conjugated secondary antibodies: goat anti-rabbit 488 (Abcam, ab150077), goat anti-guinea pig 555 (Abcam, ab150186) and donkey anti-mouse 647 (Abcam, ab150107); always in 1:1000 dilution, and with DAPI in 1:1000, for 2 h in dark. Afterwards, the sections were washed three times in PBS, each for 10 mins, in dark. Finally, the sections were mounted on glass slides with mounting media to preserve fluorescence (CSH, 2006) and stored at 4 ºC in dark.

Organotypic hippocampal slice culture preparation

In order to address stress induced molecular changes in a more controllable/standardizable conditions, an experiment on hippocampal slice cultures was performed. Preparation of organotypic hippocampal slice cultures followed procedures described by Stoppini et al. (1991) with modifications as detailed below. Hippocampi from 7-day old Sprague-Dawley rat pups were aseptically removed and placed into dissecting medium (Hanks' balanced salt solution (HBSS) medium without calcium and magnesium; Gibco™, 14170112). Using a McIllwain tissue chopper (Mickle Laboratory Engineering Co. Ltd.), each hippocampus was coronally sectioned at 350 µm and placed into fresh culture medium. Culture medium is composed of 45 % Minimum Essential Media (MEM; Gibco™, numero de catálogo), 25 % Earle's Balances Salt Solution (EBSS; Gibco™, 24010043), 25 % Horse Serum, 2% B27 supplement, 32.5 % glucose, 1 % penicillin/streptomycin, 2 µM FdU, and 2 µM uridine. Three slices were transferred onto individual Millicell-CM 0.4 µm biopore membrane inserts (Merk Millipore, PICM0RG50) and then placed in 35 mm six-well culture plates containing 1 ml of pre-incubated culture medium. Excess medium on top of slices was aspirated to ensure cultures remained exposed to the atmosphere of 5% CO2/95% air in a CO_2 incubator (Heracell™ 150i CO_2 Incubator, Thermo Scientific™, 51026406). Cultures were kept at 37 °C in an incubator at 95 % humidity and were allowed to become attached to membrane inserts for 8 days prior to the start of experiments.

Dexamethasone administration and immunohistochemistry

At 8 days in vitro, the medium of cultures (*n*=6/group) was replenished with culture medium containing either vehicle (methanol) for control group or dexamethasone (Dex; 100 µM) for two different stress groups. Soon after, cultures were placed again in the CO_2 incubator. 6 h later, a group of cultures (hereafter named 6h-Dex) with Dex was transferred to plates containing PBS and washed with PBS 3 times to remove Dex. This exposure time was selected as a trace for early changes in gene expression induced by Dex. Then, the cultures were fixed in 4 % paraformaldehyde for 30 mins (adding 1 ml PFA above and 1 ml PFA below each insert) and subsequently washed with PBS (3 washes). The slices were kept in PBS 0.2 % sodium azide at 4 ºC. The remaining cultures where fixed following the same procedure 24 h after Dex was applied (what makes this group to be referred as 24h-Dex). This exposure time represents a more prolonged chronic stress condition.

Note that unlike in the case of acute stress animal model, these organotypic slices are to be defined as a chronic stress model, keeping in mind the large duration of Dex (6 and 24 h) in the culture medium.

Once all slices were fixed, immunohistochemistry with the same primary and secondary antibody sets used for animals was performed, primarily following the protocol defined by Gogolla et al. (2006). Briefly, permeabilization and blocking of the tissue was performed with 5 % BSA and 0.5 & Triton X-100 in PBS solution, overnight at 4 ºC. The membranes were then carefully cut off from the inserts with the help of forceps and scalpel and placed in a humidity incubation box on top of plastic covers (slices facing up). The primary antibodies (against CR, PV and NDMAR1) were prepared in the blocking solution, each at 1:250 concentration. 80 µl of the primary antibodies solution were put onto each membrane, and incubated overnight at 4 ºC in the closed humidity incubation box. Then, the slices were transferred on the covers to 6-well plates (one membrane per well), letting the cover sink in the well beneath the membrane. Slices where washed three times with PBS, for 10 mins each. Next, as PBS was removed membranes were let to stick to the top of the covers that where at the bottom of the well. The membranes were transferred again on the covers to the humidity incubation box. For the incubation of the secondary antibodies, 80 µl (1:1000 dilution each with DAPI in 1:1000) was added onto de slices. The humidity incubation box was kept closed at room temperature at dark for 4 h. Washes of the secondary antibodies were realized in the same way as for the primaries. Whole membranes with the stained slices facing up were mounted on glass slides with mounting media to preserve fluorescence (CSH, 2006) and stored at 4 ºC in dark.

Image acquisition

Images were acquired using a 20x objective lens on a Leica Stellaris 5 confocal microscope using the Las X Navigator module to acquire a TileScan image of the regions of interest (ROIs). Z-stacks were obtained to visualize section in depth. For every ROI a pile of 12 slices made the z-stack, spaced by a distance of 1.9 µm. For image analysis 5 consecutive slices were chosen manually which yielded on a 7.6-µm-thick brain section.

The confocal settings were kept constant all along the imaging process to preserve the comparability among images. Parameters concerning the captured signal, e. g., the gain and the intensity, were set to obtain a signal halfway to maximum intensity value, to avoid saturation and ensure full conservation of the signal. A 405 nm diode and a white laser were used for excitation of the fluorophores, adjusting the excitation wavelengths to each fluorophore. A hybrid detector was assigned to each channel, with the proper wavelength windows to avoid fluorescence crosstalk (Table 1).

Table 1. Settings for image acquisition in the confocal microscope.

Detector (wavelength window)	Laser line	PrL, CA1, BLA of rats		NaC of rats		CA1 of hipp. slices	
		Gain	Intensity	Gain	Intensity	Gain	Intensity
HyD S1 (658 nm - 766 nm)	653 nm	5	16 %	5	16 %	4	13 %
HyD S2 (560 nm - 627 nm)	553 nm	6	4 %	4	2 %	2	0.4 %
HyD S3 (495 nm - 557 nm)	490 nm	4	4.5 %	4	4.5 %	3	6.3 %
HyD S3 (420 nm - 506 nm)	405 nm	2	2.5 %	2	2.5 %	2	2 %

HyD: hybrid detector; BLA; basolateral amygdala; CA1: *cornus ammonis* 1; PrL: prelimbic cortex; NaC: nucleus accumbens. BLA, CA1 and PrL brain area images were acquired with the same confocal settings. To image NaC settings were reset to avoid saturation since the signal intensity relative to other areas was considerably higher.

Computer-assisted image analysis

Digital images are data. This allows image analysis to be operated by computers, offering unbiased processing of the information and perfect reproducibility. For this reason, we focused on developing a workflow with computer programs to extract the information of interest, avoiding the experimenter's subjectivity to the greatest degree possible. Several software was used to accomplish the analysis. For the first step, Fiji-ImageJ (1.53c; Schindelin et al. 2012; Schneider et al., 2012), a broadly used software in biological science, was the main tool for the extraction of specific information including cell count and signal

intensity. Likewise, Python (3.9.7; Van Rossum and Drake, 1995) scripts helped organizing and restructuring the output obtained from Fiji-ImageJ. Finally, R software (4.2.0, 2022-04-22 ucrt; R Core Team 2022) was used for statistical analysis (detailed in the next section).

The process was designed to get information about cell density and changes in signal intensity of the somas. Precisely, the analysis can be understood in two parts: i) the quantification of the number and signal intensity of PV+ and CR+ cells, and ii) the colocalization with NMDAR1 signal within those cells. Three aspects or variables were obtained from each of the parts, as described below. To accomplish that, Fiji-ImageJ macros were built, which permitted automation of the process over all images (find the macros in Supplementary information).

For the first part, on which CR and PV channels were analyzed, a key main function of the macros consists on creating selections outlining signal-positive cells. A well-known tool to do that in ImageJ is the "Analyze particles" command, which creates a set of ROIs surrounding objects with a pixel value over a threshold. "Analyze particles" works by scanning the image until it finds the edge of the object with the defined threshold. The drawback with that method is that in a sample where cells display different intensities of fluorescence, it is challenging to find a threshold where all and exclusively the cells are outlined: there may be cells or areas of cells with pixel values below the threshold led outside the selection (Fig. 1a) and/or areas inside the selection not belonging to the structure of the cell (Fig. 1b).

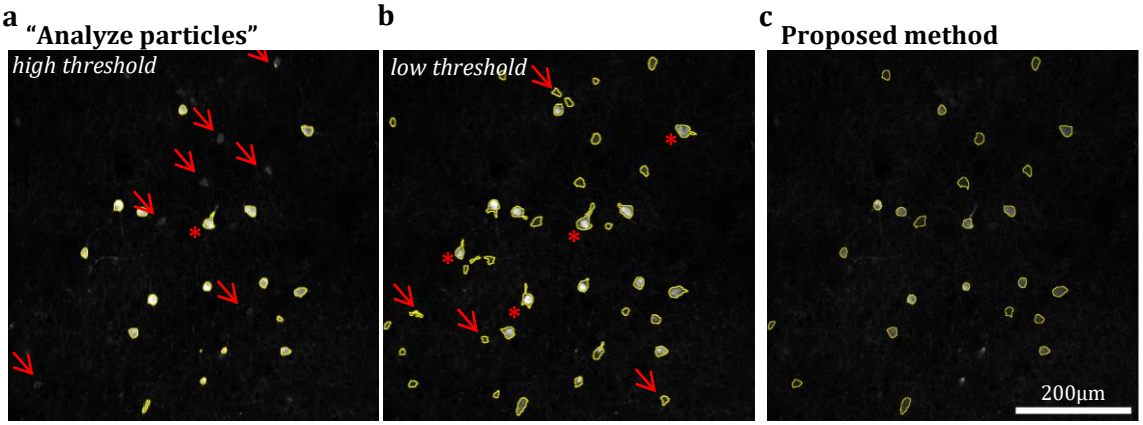

Figure 1. "Analyze particles" vs. proposed method. It is an image of BLA of an stressed rat, labelled for calretinin. On image **a** a relatively high threshold was applied for "Analyze particles" method, and indicated by an arrow are the cells the method failed to be selected (or are partially selected) due to their low intensity values that were led under the threshold. On image **b** a relatively low threshold was set for "Analyze particles" method, on which arrows indicates structures that are not somas the method selected because they display an intensity over the threshold. Asterisks (*) always indicate selections that contain structures other than somas. Note that the proposed method (image **c**) selects just the somas and all the somas, efficiently outlining the edge of the structure.

Outlining the whole cell body accurately is a prerequisite to assess its overall fluorescence intensity. Hence, an alternative to "Analyze particles" was developed. For this purpose, we took advantage of "Find Maxima" and "Wand Tool" commands. After some basic preliminary image processing (background subtraction, application of filters…) "Find Maxima" was run for identifying pixels displaying maximum of luminance (the so-called *maxima*), with a determined *prominence* threshold. Afterwards, the macro runs the "Wand Tool" through every *maximum*, which selects a contiguous area under the condition that all pixel values in that area must be in the range *initial value – tolerance* to *initial value + tolerance*. In our images, signal intensity inside somas is quite homogeneous, with a gradual

decline towards the edges. Thus, for different *maxima* a given *tolerance* threshold leads to different selections for every cell. Yet, it was found that a fixed ratio between the value of the *tolerance* and the *maximum* would outline the cell soma regardless of the value of the *maximum*, making it possible to run a *maximum*-dependent tolerance value for each *maximum* (Fig. 1c; Table 2). In a nutshell, the aim is to run "Find Maxima" command with an optimal *prominence* threshold to select a single *maximum* in each cell, and next run the "Wand Tool" over the *maxima* with the *tolerance* value that fits the stablished *tolerance/maximum* ratio for the cell soma selection in each case.

Table 2. Parameters for creating (with Fiji-ImageJ) and filtering (in Python) cell selections.

Cell soma selecting parameters	rats CR channel	rats PV channel	hippo. slices CR channel	hippo. slices PV channel
Prominenece threshold	5000	6000 (exc: CA1 10000)	5000	5000
Tolerance/Maximum ratio	0.65	0.65 (exc: CA1 0.55)	0.55	0.25
Area filter (μm^2)	>60, <1000	>75, <1000	>50, <1000	>20, <200
Circularity filter	0.55	0.65	0.60	0.60

Hippo.: hippocampal; CR: calretinin; PV: parvalbumin.

After obtaining the cell soma outlines, parameters such as area, shape descriptors and the integrated density were measured in every cell selection. Cell selections were filtered by circularity and area to exclude unspecific selections using Python (see Table 2). Equally, Python facilitated the calculations of the three variables obtained out from the ImageJ-Fiji data:

Cell density. We calculated the neuronal densities using the following formula as reported earlier (Gabbot et al., 1997): the number of counted cells was divided by the volume of the brain area and expressed as cell-number/mm^3 volume.

Mean CTCF. CTCF stands for "corrected total cell fluorescence" and is defined by the formula *CTCF* = *integrated density* - (*cell area* × *background mean pixel value*) [A.U.] (El-Sharkawey, 2016). The average CTCF was calculated for each cell selection, thus, this variable is a measure of the mean CTCF value of an analyzed tissue area. The mean CTCF gives a sense of the average marker expression (or fluorescence intensity) the cells of an analyzed image display.

Standard deviation (SD) of the mean CTCF. This variable is a measure of the standard deviation of the mean CTCF of an analyzed tissue area. It is meant to provide information on the variability of CTCF values within the area; i.e., the range of the marker expression level of the cells. Most of the cells may have same CTCF value (low SD), or there may be huge differences on the CTCF values (high SD).

For the second part regarding the colocalization analysis in Fiji-ImageJ, NMDAR1 signal was studied in both CR and PV channels independently. For that matter, the outlines of CR or PV were displayed (case-by-case) onto NMDAR1 channel and measured NMDAR1 signal in those selections (Fig. 2). Again, three variables were extracted from these data using Python:

Percentage of NMDAR1 expressing CR+ or PV+ cells. CTCF values of NMDAR1 within CR+ or PV+ cell selections were calculated. A threshold of 5000 units for CTCF of NMDAR1 was set to consider the cell as NMDAR1+.

CTCF mean of NMDAR1 in CR+ or PV+ cells. The mean of NMDAR1 CTCF of all the CR+ or PV+ cell selections of an analyzed tissue area.

CTCF SD of NMDAR1 in CR+ or PV+ cells. The standard deviation of the NMDAR1 CTCF mean of the CR+ or PV+ cells of an analyzed tissue area. This variable is meant to provide information on the variability of NMDAR1 CTCF values within the tissue area as previously explained in the first part of the analysis.

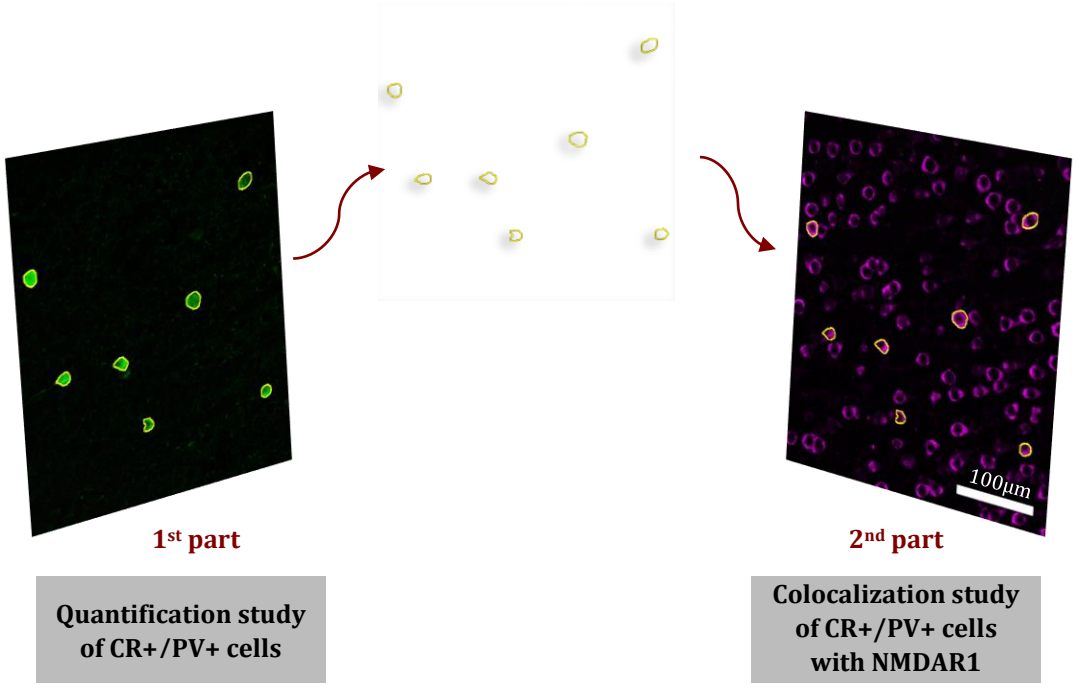

Fig. 2. A general visual representation of the image analysis workflow. In the first part of the analysis soma selections are created for the quantification study of CR+ or PV+ cells (in the figure calretinin is displayed). In the second part the outlines obtained in the first part are superposed in NMDAR1 channel images. These images are of the prelimbic cortex of a stressed rat. CR: calretinin; PV: parvalbumin.

Oftentimes, while analyzing images the experimenter chooses a ROI which comprises a specific area of interest instead of analyzing the whole original image that may contain other parts not belonging to the area of interest. At the beginning of this workflow the macros permit, if needed, interacting with the experimenter to select a ROI of the specific brain area, whose position is adjustable to the image in each case by the experimenter's criteria (Fig. 3).

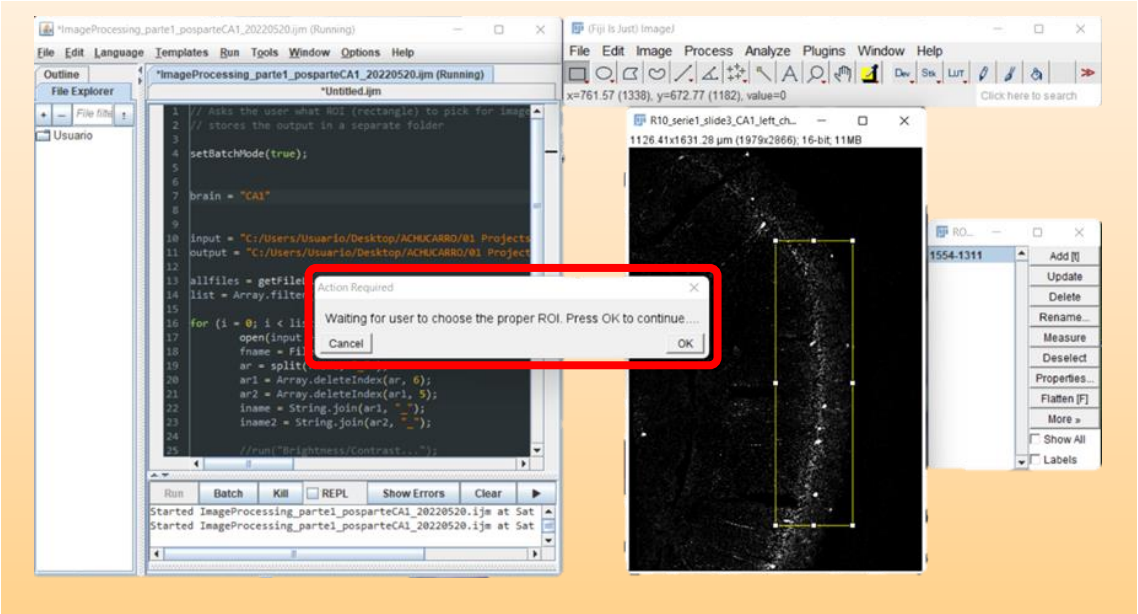

Fig. 3. Snapshot of the user interaction of a running the macro. The rectangle in red show the window that sets the interaction with the user, so the user can choose the region of interest moving the position of the rectangle in yellow.

The workflow was executed in all images of the brain areas of interest (PrL, NaC, BLA and CA1) of the rats plus CA1 of the organotypic hippocampal slices. All details of image processing are determined in the codes (Fiji-ImageJ and Python) themselves (see Supplementary information).

Statistical analysis

To test whether statistically significant differences exist between stressed and not-stressed groups of rats Student's unpaired *t*-test was applied. In the case of hippocampal organotypic slices, one-way analysis of variance (ANOVA) was the chosen test, followed by Tukey's honestly significant difference (HSD). Results are presented with p-values, estimates and 95 % confidence intervals (CIs). Statistical significance is considered for *p*-values below 0.05, although up to 0.1 biological importance was credited. These statistical tests assume groups being compared present homogeneous data, both being normally distributed and having equal variances. For small samples as the ones on hands, statistical tests to check these features are not reliable, herein, descriptive statistics have been used: normality was assessed by normal QQ plots, while equality of variances and homogeneity were examined displaying boxplots and violinplots. Statistical analysis was carried out in R (2021.9.1.372), using the following packages: "extrafont" (Chang, 2022), ,"ggsci" (Xiao, 2018), "ggplot2" (Wickham et al., 2016), "ggprism" (Dawson, 2021), "ggpubr" (Kassambra, 2020), "gridExtra" (Auguie, 2017),"readxl" (Wickham et al., 2019), "see" (Lüdecke et al., 2021), "tidyverse" (Wickham et al., 2019), "xlsx" (Dragulescu and Arendt, 2020).

RESULTS

Stress decreases parvalbumin expression in CA1 of rats

In the acutely stressed rat model in respect to parvalbumin expression, there is an estimated 906345 units decrease of the mean CTCF, that is, 27 % of decrease (*p*-value = 0.028, 95 % CI = 109338–1703352; Fig. 4). No changes in CR+ cell density was contemplated. The variability of CTCF values (as given by the SD of the mean of CTCF) did not change neither, concluding that in both groups (stressed and not-stressed) the expression levels extended to the same range.

Stress decreases calretinin expression in BLA of rats

Expression of the markers can change in different aspects: in cell number, intensity (mean CTCF), and distribution of the expression level among cells (SD CTCF). From the analysis of the CR marker in BLA of the rats, a decrease of the CR expression was found in stressed rats. The unpaired *t*-test estimated that the mean CTCF decreased 230322 units, which is a decrease of the 21 % (*p*-value = 0.045, 95 % CI = 5245–455397; Fig. 4). Nonetheless, no changes in CR+ cell density was contemplated. The variability of CTCF values (as given by the SD of the mean of CTCF) did not change neither, concluding that in both groups (stressed and not-stressed) the expression levels extended to the same range.

Stress alters parvalbumin expression in CA1 in hippocampal slices

As in CA1 of rats, a decrease in mean CTCF can also be seen in hippocampal organotypic slices treated 24 h with Dex comparing with control group, being the estimated difference 52873, 35 % decrease (*p*-value = 0.097, 95 % CI = -8689–114435; Fig. Sb). In spite the decrease in mean CTCF, the number of PV+ cells increases by 14378314 cells/mm^3 estimation, what is a 62 % of increment (*p*-value = 0.026, 95 % CI = 1698688–27057940

[cells/mm^3]; Fig. Sc). The SD of the mean CTCF (the variability of the PV signal) is reduced 52 % in 24h-Dex compared to control, to an estimated value of 86424 (p-value = 0.053, 95 % CI = 1325–189308; Fig. 5).

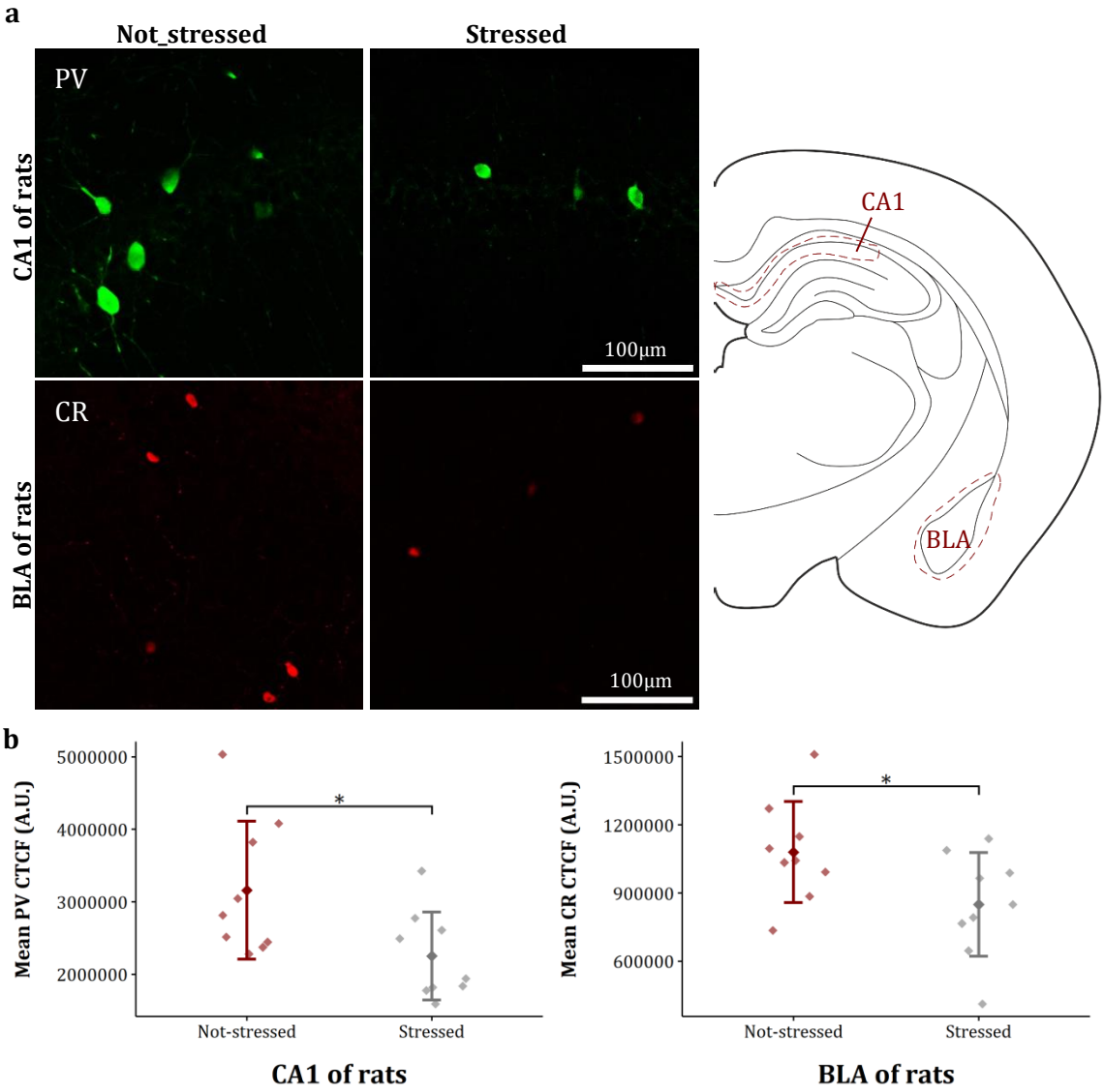

Fig. 4. Changes in parvalbumin and calretinin expression in the rat model of acute stress. a Confocal fluorescence images of stressed and not stressed rats of the brain areas (BLA and CA1) where alterations in parvalbumin (PV) and calretinin (CR) expression were found. **b** We found a decrease in the mean corrected total cell fluorescence (CTCF) in CA1 of stressed rats; and that they also display minor mean CTCF value in basolateral amygdala (BLA; Student's unpaired t-test, $n_{Not\text{-}stressed}$=9, $n_{Stressed}$=10). Data is shown with mean and standard deviation bars. *p> 0.5.

Stress increases calretinin expression in the CA1 of hippocampal slices

In hippocampal slices, there is a tendency of CR expression to increase from the 6h-Dex group to the 24h-Dex. Differences in the mean CTCF with an estimation of 1300637 units was found, understood as the 50 % of increment (adj. p-value = 0.014, 95 % CI = 274024–2327250; Fig. 5). No changes in CR+ cell density was contemplated. The variability of CTCF values (as given by the SD of the mean of CTCF) did not change neither, concluding

that in both groups (stressed and not-stressed) the expression levels extended to the same range.

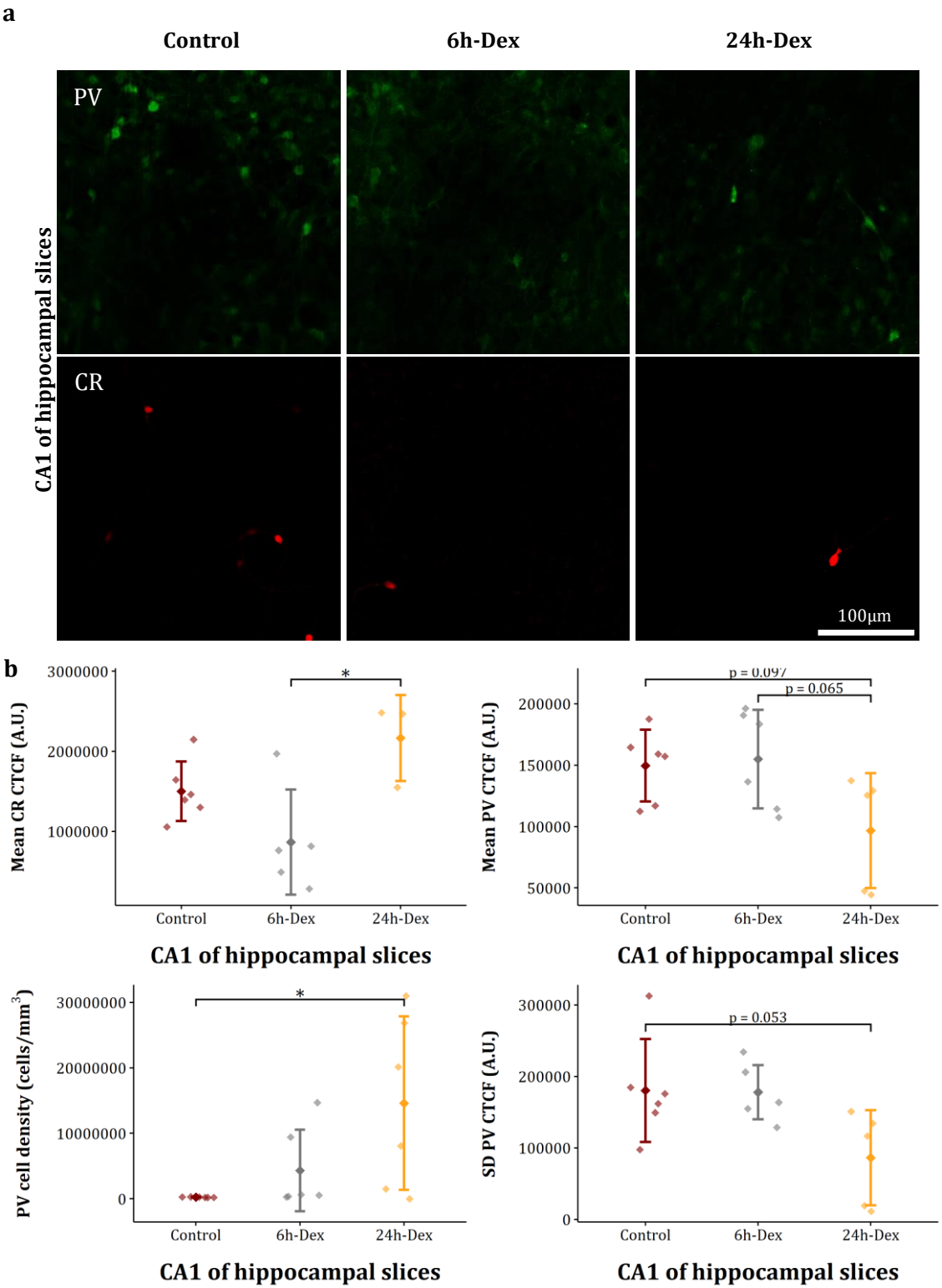

Fig. 5. Changes in parvalbumin and calretinin expression in organotypic rat hippocampal slice model of chronic stress. a Confocal fluorescence images of rat hippocampal slices (CA1 region) treated with vehicle (control), or with dexamethasone (Dex) for 6 h (6h-Dex) and 24 h (24h-Dex) labelled for parvalbumin (PV) and calretinin (CR). **b** We found an increase in the mean corrected total cell fluorescence (CTCF) in 24h-Dex

compared to 6h-Dex, and a gradual decrease of the mean CTCF of PV, although an increase in the PV+ cells density and a decrease in standard deviation (SD) of CTCF of PV (one way ANOVA, n=6 slices/group). Data is shown with mean and standard deviation bars. *p> 0.5.

Stressed did not alter NMDAR1 expression in the rat model nor in hippocampal slices

We did not find any difference in stress conditions while analysing the NMDAR1 expression of the CR+ or PV+ cells (case-by-case), not in animals nor in the organotypic hippocampal slices (data not shown).

Table 3. A summary of the statistics: results of Student's unpaired t-tests for animal experiments and Tukey's HSD tests for hippocampal slices.

	Animals		
Variables	Not-stressed (n = 9)	Stressed (n = 10)	ED (95 % CI) *p* -value
BLA, mean CR CTCF (SD)	1080580 (222144)	850258 (228266)	230322 (5245; 455397) 0,045
CA1, mean PV CTCF (SD)	3160036 (950839)	2253691 (606665)	906345 (109338; 1703352) 0,028
	Hippocampal slices		
Variables	Group 1 (n = 6)	Group 2 (n = 6)	ED (95 % CI) adj. *p* -value
	6h-Dex	*24h-Dex*	
CA1, mean CR CTCF (SD)	865718 (655179)	2166355 (535811)	-1300637 (-2327250; -274024) 0,014
	control	*24h-Dex*	
CA1, PV cell density (SD)	232573 (47478)	14610887 (13253810)	-14378314 (-27057940; -1698688) 0,026
	control	*24h-Dex*	
CA1, mean PV CTCF (SD)	149575 (29249)	96702 (46787)	52873 (-114434; 8688) 0,097
	6h-Dex		
	154926 (154926)		58223 (-3338; 119785) 0,065
	control	*24h-Dex*	
CA1, SD PV CTCF (SD)	180416 (71876)	86424 (66425)	93992 (1325; 189308) 0,053

ED: estimated difference; CI: confidence interval; SD: standard deviation; CR: calretinin; PV: parvalbumin; CTCF: corrected total cell fluorescence; Dex: dexamethasone, BLA: basolateral amygdala; CA1: *cornus ammonis* 1.

DISCUSSION

Experiments performed with the animal model and the organotypic hippocampal slices altogether offer a general overview of the internal mechanisms of stress, from acute to chronic forms. Stress-related disorders involve complex cellular and molecular changes, and GABAergic signalling is currently being addressed as an important system in the field. In the present work we attempt to immunohistochemically map the CR and PV changes caused by stress and to address the stress-associated learning impairment by labelling NMADR1, involved in LTP.

Regarding the results from the animals of the acute stress model, from all the analyzed brain areas, molecular changes were only found in BLA and CA1 of the hippocampus. In these areas GABAergic cells give rise to about 20 % of the total neuronal population (Hájos. 2021). Many of them are calcium binding proteins such as parvalbumin (PV) and calretinin (CR), that buffer intracellular calcium concentrations in neurons and thereby modulate calcium transients in activated neurons (Schwaller, 2012; Albrecht et al., 2021).

In the case of the BLA, an estimated increase of the 21 % in the mean CTCF of CR was found in stressed rats. Predominant cells expressing CR in the BLA are small non-pyramidal interneurons with a bipolar or bitufted dendritic arborization pattern, which form synapses with the most proximal part of excitatory and inhibitory neurons (McDonald, 1994). As earlier reported, CR immunoreactivity in BLA is not only located in local circuit neurons, but also in neurons that connect the amygdaloid complex with other brain areas (Sorvari et al., 1996). In fact, an interesting efference is the anterior BLA that innervates the deep-layer calbindin1-negative neurons in ventral CA1. Pi and co-workers (2020) showed that stimulating that exact BLA-CA1 connection in mice induces anxiety-like behaviour resulting in fewer approaches. Perhaps, this discovery could be an explanation to the impaired learning ability (slower learning) of the stressed rats from the present work. It could be the case that the decrease in mean CTCF of PV in CA1 could be an extended effect of the decrease in mean CTCF of CR in BLA triggered by the BLA-CA1 projection, resulting in the failure of animals to accomplish the tasks as Pi and co-workers described. Of course, such a hypothesis would need further research.

To continue with the results of animal experiments, as already mentioned, the CA1 of the stressed rats experienced a decline in the mean CTCF of PV, by a magnitude of 27 %. PV within the hippocampus is predominantly found in so-called basket cells. Referring to their morphological appearance, basket cells extensively contact excitatory cells at the soma or the proximal part of the dendrites to provide perisomatic inhibition. Basket cells are connected by inhibitory synapses and by gap junctions that allow for a fast coupling of their activity (Traub et al., 2001). With their fast-spiking pattern, they control rhythmical activity of pyramidal cells (Bartos et al., 2007). The decrease in intracellular expression of PV may be detrimental, negatively interfering with the pyramidal cell functions. Some stated that low PV via a reduction in the intracellular calcium-buffering capacity may increase the vulnerability to excitotoxicity (Vanselow and Keller, 2000). For example, in an animal model of motor neuron disease, neurons expressing high levels of PV were particularly resistant to excitotoxicity (Elliott and Snider, 1995) and mice overexpressing PV were more resistant to cell death (Dekkers et al., 2004). Whether similar processes occur in the hippocampus remains to be elucidated in future studies (Filipović et al., 2013).

Regarding the organotypic hippocampal slices (our chronic stress model) higher levels of mean CTCF of CR were detected in the CA1 of 24h-Dex group, precisely, a 50 % of increment. In the hippocampus, the CR+ interneurons innervate calbindin-containing interneurons as well as vasoactive intestinal peptide (VIP)-containing basket cells. This way, CR+ interneurons may participate generating synchronous, rhythmic hippocampal activity by controlling other interneurons that establish axodendritic and axosomatic

synapses with principal cells (Gulyas et al., 1996). Reduce concentration of calcium-buffering proteins may likely reflect a functional impairment (Czeh et al., 2018).

PV expression changes in several aspects in the CA1 of chronically stressed hippocampal slices. There is a decrease of the mean CTCF of PV by a 27 % as seen in CA1 of acutely stressed rats. Despite the lower average PV intracellular expression, we found a higher PV+ cell density in Dex-24h (62 % higher). And SD of the mean CTCF was reduced down to a 35 %, what indicates a lower variability in intracellular expression among cells, i.e., most of the cells display a lower and more similar value than those of the control group. Again, reduced cytoplasmic protein expression may compromise the vulnerability to excitotoxicity (Vanselow and Keller, 2000), but, in this case, increased PV+ cell density may indicate a compensatory molecular response.

Chronic stress is more well-documented in the literature than acute stress, specially respecting to the hippocampal structures. There is unanimity while highlighting stress-related GABAergic dysfunction. Nevertheless, regarding alterations in interneuron markers the results are heterogeneous, and the mechanism underlying those changes and the downstream consequences are not fully understood. For example, contrary to what we have observed, others have reported a decrease in the density of CA1 PV+ cells in Dex-treated rat hippocampal slices (Hu et al., 2010), chronic mild stress (CMS) rat model (Czeh et al., 2015), chronically stressed rats (Filipovic et al., 2013), socially isolated rats (Filipovic et al., 2017) and in a mouse model of adolescent chronic social stress (Wang et al., 2019); while others did not find any change at all studying psychosocial stress (Czeh et al., 2005).

To what molecular learning mechanisms concern, we did not find NMDAR1 changes linked to stress, not in the animal model that showed learning impairment in the Skinner box test, and neither in the organotypic hippocampal slices. The reason why NMDAR1 remains the same in the case of hippocampal slices is not surprising, as no learning-like changes were externally induced to the cultures. Hence, there was no stimuli to elicit alteration in the NMDAR expression. Similarly, NMDAR1 showed no difference in the acute stress group of rats. This seems logic if we remember that by the end of the Skinner box test, both groups of rats (stressed and control) performed equally. Most probably, changes were to be found at the beginning of the test, where stressed rats showed lower performance.

It is known since long ago that high levels prolonged exposure of corticosterone (a glucocorticoid) due to stress suppresses LTP (Kerr et al., 1994; Alfarez et al., 2003). In addition, LTD can be facilitated in animals exposed to chronic stress (Yang et al., 2006; Ma et al., 2007). Exposure to such corticosterone concentrations activates both MRs and GRs. Most of the documented negative impacts have been observed hours after corticosterone application (Krugers et al., 2005; Wiegert et al., 2005), suggesting the requirement of GR-induced genomic mechanisms (Tsai and O'Malley, 1994). The detrimental impacts of corticosteron on memory functions could be partly attributed to GR-mediated LTP suppression. LTP is suppressed by GR agonists (Pavlides et al., 1995) and stress-induced inhibition of LTP is blocked by GR antagonists (Avital et al., 2006). Anyhow, contrary to what our collaborators observed in the stressed rats, other studies suggest that acute stress may improve cognitive processes under certain conditions (Yuen et al., 2011) and associative learning in a glucocorticoid-dependent manner (Beylin and Shors, 2003).

In summary, the susceptibility of PV and CR neurons to stress may represent a key mechanism contributing to functional and structural deterioration in specific brain regions, such as the CA1 of the hippocampus or the BLA. Such nuclei are certainly prone to be associated with psychiatric illness, especially true for stress-related disorders such as PTSD and depression. Further research on PV and CR alterations may open a door to a novel and important strategy to promote resilience against stress-related disorders in the future. In this respect, our data provide information to the increasingly growing field of the interneuron interplay in stress.

ACKNOWLEDGEMENTS

We would like to thank to Prof. Jose María Delgado García and Prof. Agnés Gruart i Massó from Division of Neurosciences at Pablo de Olavide University in Seville, Spain, for performing the behavioural and electrophysiology experiments in the stressed rats and for providing their brains for this work.

REFERENCES

Akirav, I., & Richter-Levin, G. (2002). Mechanisms of amygdala modulation of hippocampal plasticity. *The Journal of neuroscience : the official journal of the Society for Neuroscience*, *22*(22), 9912–9921. https://doi.org/10.1523/JNEUROSCI.22-22-09912.2002.

Albrecht, A., Redavide, E., Regev-Tsur, S., Stork, O., & Richter-Levin, G. (2021). Hippocampal GABAergic interneurons and their co-localized neuropeptides in stress vulnerability and resilience. *Neuroscience and biobehavioral reviews*, *122*, 229–244. https://doi.org/10.1016/j.neubiorev.2020.11.002.

Alfarez, D. N., Joëls, M., & Krugers, H. J. (2003). Chronic unpredictable stress impairs long-term potentiation in rat hippocampal CA1 area and dentate gyrus in vitro. *The European journal of neuroscience*, *17*(9), 1928–1934. https://doi.org/10.1046/j.1460-9568.2003.02622.x.

Auguie B (2017). _gridExtra: Miscellaneous Functions for "Grid" Graphics_. R package version 2.3, https://CRAN.R-project.org/package=gridExtra.

Avital, A., Segal, M., & Richter-Levin, G. (2006). Contrasting roles of corticosteroid receptors in hippocampal plasticity. *The Journal of neuroscience : the official journal of the Society for Neuroscience*, *26*(36), 9130–9134. https://doi.org/10.1523/JNEUROSCI.1628-06.2006.

Bartos, M., Vida, I., & Jonas, P. (2007). Synaptic mechanisms of synchronized gamma oscillations in inhibitory interneuron networks. *Nature reviews. Neuroscience*, *8*(1), 45–56. https://doi.org/10.1038/nrn2044.

Berardi, A., Trezza, V., Palmery, M., Trabace, L., Cuomo, V., & Campolongo, P. (2014). An updated animal model capturing both the cognitive and emotional features of post-traumatic stress disorder (PTSD). *Frontiers in behavioral neuroscience*, *8*, 142. https://doi.org/10.3389/fnbeh.2014.00142.

Beylin, A. V., & Shors, T. J. (2003). Glucocorticoids are necessary for enhancing the acquisition of associative memories after acute stressful experience. *Hormones and behavior*, *43*(1), 124–131. https://doi.org/10.1016/s0018-506x(02)00025-9.

Calogero, A. E., Gallucci, W. T., Chrousos, G. P., & Gold, P. W. (1988). Catecholamine effects upon rat hypothalamic corticotropin-releasing hormone secretion in vitro. *The Journal of clinical investigation*, *82*(3), 839–846. https://doi.org/10.1172/JCI113687.

Czeh, B., Simon, M., van der Hart, M. G., Schmelting, B., Hesselink, M. B., & Fuchs, E. (2005). Chronic stress decreases the number of parvalbumin-immunoreactive interneurons in the hippocampus: prevention by treatment with a substance P receptor (NK1) antagonist. *Neuropsychopharmacology : official publication of the American College of Neuropsychopharmacology*, *30*(1), 67–79. https://doi.org/10.1038/sj.npp.1300581.

Czéh, B., Vardya, I., Varga, Z., Febbraro, F., Csabai, D., Martis, L. S., Højgaard, K., Henningsen, K., Bouzinova, E. V., Miseta, A., Jensen, K., & Wiborg, O. (2018). Long-Term Stress Disrupts the Structural and Functional Integrity of GABAergic Neuronal Networks in the Medial Prefrontal Cortex of Rats. *Frontiers in cellular neuroscience*, *12*, 148. https://doi.org/10.3389/fncel.2018.00148.

Chang W (2022). _extrafont: Tools for Using Fonts_. R package version 0.18, https://CRAN.R-project.org/package=extrafont.

Cold Spring Harbor (2006). Mowiol mounting medium. *Cold Spring Harbor Protocols, 2021*(6). https://doi.org/10.1101/pdb.rec10255.

CorelDRAW Graphics Suite (RRID:SCR_014235)

Dawson, C. (2021). ggprism: A 'ggplot2' Extension Inspired by 'GraphPad Prism'. R package version 1.0.3. https://CRAN.R-project.org/package=ggprism.

Dekkers, J., Bayley, P., Dick, J. R., Schwaller, B., Berchtold, M. W., & Greensmith, L. (2004). Over-expression of parvalbumin in transgenic mice rescues motoneurons from injury-induced cell death. *Neuroscience*, *123*(2), 459–466. https://doi.org/10.1016/j.neuroscience.2003.07.013.

Dragulescu, A., & Arendt, C. (2020). xlsx: Read, Write, Format Excel 2007 and Excel 97/2000/XP/2003 Files. R package version 0.6.5. https://CRAN.R-project.org/package=xlsx.

Elliott, J. L., & Snider, W. D. (1995). Parvalbumin is a marker of ALS-resistant motor neurons. *Neuroreport*, *6*(3), 449–452. https://doi.org/10.1097/00001756-199502000-00011.

El-Sharkawey, Ayman. (2016). Calculate the Corrected Total Cell Fluorescence (CTCF). https://doi.org/10.13140/RG.2.1.1307.8008.

Filipović, D., Stanisavljević, A., Jasnić, N., Bernardi, R. E., Inta, D., Perić, I., & Gass, P. (2018). Chronic Treatment with Fluoxetine or Clozapine of Socially Isolated Rats Prevents Subsector-Specific Reduction of Parvalbumin Immunoreactive Cells in the Hippocampus. *Neuroscience*, *371*, 384–394. https://doi.org/10.1016/j.neuroscience.2017.12.020.

Filipović, D., Zlatković, J., Gass, P., & Inta, D. (2013). The differential effects of acute vs. chronic stress and their combination on hippocampal parvalbumin and inducible heat shock protein 70 expression. *Neuroscience*, *236*, 47–54. https://doi.org/10.1016/j.neuroscience.2013.01.033.

Gabbott, P. L., Dickie, B. G., Vaid, R. R., Headlam, A. J., & Bacon, S. J. (1997). Local-circuit neurones in the medial prefrontal cortex (areas 25, 32 and 24b) in the rat: morphology and quantitative distribution. *The Journal of comparative neurology*, *377*(4), 465–499. https://doi.org/10.1002/(sici)1096-9861(19970127)377:4<465::aid-cne1>3.0.co;2-0.

Giachino, C., Canalia, N., Capone, F., Fasolo, A., Alleva, E., Riva, M. A., Cirulli, F., & Peretto, P. (2007). Maternal deprivation and early handling affect density of calcium binding protein-containing neurons in selected brain regions and emotional behavior in periadolescent rats. *Neuroscience*, ç *145*(2), 568–578. https://doi.org/10.1016/j.neuroscience.2006.12.042.

Godoy, L. D., Rossignoli, M. T., Delfino-Pereira, P., Garcia-Cairasco, N., & de Lima Umeoka, E. H. (2018). A Comprehensive Overview on Stress Neurobiology: Basic Concepts and Clinical Implications. *Frontiers in behavioral neuroscience*, *12*, 127. https://doi.org/10.3389/fnbeh.2018.00127

Gogolla, N., Galimberti, I., DePaola, V., & Caroni, P. (2006). Staining protocol for organotypic hippocampal slice cultures. *Nature protocols*, *1*(5), 2452–2456. https://doi.org/10.1038/nprot.2006.180.

Gulyás, A. I., Hájos, N., & Freund, T. F. (1996). Interneurons containing calretinin are specialized to control other interneurons in the rat hippocampus. *The Journal of neuroscience : the official journal of the Society for Neuroscience*, *16*(10), 3397–3411. https://doi.org/10.1523/JNEUROSCI.16-10-03397.1996.

Hájos N. (2021). Interneuron Types and Their Circuits in the Basolateral Amygdala. *Frontiers in neural circuits*, *15*, 687257. https://doi.org/10.3389/fncir.2021.687257.

Hariri, A. R., & Holmes, A. (2015). Finding translation in stress research. *Nature neuroscience*, *18*(10), 1347–1352. https://doi.org/10.1038/nn.4111

Joëls, M., & Baram, T. Z. (2009). The neuro-symphony of stress. *Nature reviews. Neuroscience*, *10*(6), 459–466. https://doi.org/10.1038/nrn2632.

Kassambra, A. (2020). ggpubr: 'ggplot2' Based Publication Ready Plots. R package version 0.4.0. https://CRAN.R-project.org/package=ggpubr.

Kerr, D. S., Huggett, A. M., & Abraham, W. C. (1994). Modulation of hippocampal long-term potentiation and long-term depression by corticosteroid receptor activation. *Psychobiology* 22, 123–133.

Krugers, H. J., Alfarez, D. N., Karst, H., Parashkouhi, K., van Gemert, N., & Joëls, M. (2005). Corticosterone shifts different forms of synaptic potentiation in opposite directions. *Hippocampus*, *15*(6), 697–703. https://doi.org/10.1002/hipo.20092.

Lüdecke, D., Patil, I., Ben-Shachar, M.S., Wiernick, B.M., Waggoner, P., & Makowski, D. (2021). see: An R Package for Visualizing Statistical Models. Journal of Open Source Software, 6(64), 3393. https://doi.org/10.21105/joss.03393.

Lüscher, C., & Malenka, R. C. (2012). NMDA receptor-dependent long-term potentiation and long-term depression (LTP/LTD). *Cold Spring Harbor perspectives in biology*, *4*(6), a005710. https://doi.org/10.1101/cshperspect.a005710.

Ma, W. P., Cao, J., Tian, M., Cui, M. H., Han, H. L., Yang, Y. X., & Xu, L. (2007). Exposure to chronic constant light impairs spatial memory and influences long-term depression in rats. *Neuroscience research*, *59*(2), 224–230. https://doi.org/10.1016/j.neures.2007.06.1474.

McDonald A. J. (1994). Calretinin immunoreactive neurons in the basolateral amygdala of the rat and monkey. *Brain research*, *667*(2), 238–242. https://doi.org/10.1016/0006-8993(94)91501-6.

Nobili, A., Krashia, P., Cordella, A., La Barbera, L., Dell'Acqua, M. C., Caruso, A., Pignataro, A., Marino, R., Sciarra, F., Biamonte, F., Scattoni, M. L., Ammassari-Teule, M., Cecconi, F., Berretta, N., Keller, F., Mercuri, N. B., & D'Amelio, M. (2018). Ambra1 Shapes Hippocampal Inhibition/Excitation Balance: Role in Neurodevelopmental Disorders. *Molecular neurobiology*, *55*(10), 7921–7940. https://doi.org/10.1007/s12035-018-0911-5.

Pavlides, C., Watanabe, Y., Magariños, A. M., & McEwen, B. S. (1995). Opposing roles of type I and type II adrenal steroid receptors in hippocampal long-term potentiation. *Neuroscience*, *68*(2), 387–394. https://doi.org/10.1016/0306-4522(95)00151-8.

Pi, G., Gao, D., Wu, D., Wang, Y., Lei, H., Zeng, W., Gao, Y., Yu, H., Xiong, R., Jiang, T., Li, S., Wang, X., Guo, J., Zhang, S., Yin, T., He, T., Ke, D., Li, R., Li, H., Liu, G., Yang, X., Luo, M. H., Zhang, X., Yang, Y., & Wang, J. Z. (2020). Posterior basolateral amygdala to ventral hippocampal CA1 drives approach behaviour to exert an anxiolytic effect. *Nature communications*, *11*(1), 183. https://doi.org/10.1038/s41467-019-13919-3.

R Core Team (2022). R: A language and environment for statistical computing. R Foundation for Statistical Computing, Vienna, Austria. URL https://www.R-project.org/.

Schindelin, J., Arganda-Carreras, I., Frise, E., Kaynig, V., Longair, M., Pietzsch, T., Preibisch, S., Rueden, C., Saalfeld, S., Schmid, B., Tinevez, J. Y., White, D. J., Hartenstein, V., Eliceiri, K., Tomancak, P., & Cardona, A. (2012). Fiji: an open-source platform for biological-image analysis. *Nature methods*, *9*(7), 676–682. https://doi.org/10.1038/nmeth.2019.

Schneider, C. A., Rasband, W. S., & Eliceiri, K. W. (2012). NIH Image to ImageJ: 25 years of image analysis. *Nature methods*, *9*(7), 671–675. https://doi.org/10.1038/nmeth.2089.

Schwaller, B. (2012). The use of transgenic mouse models to reveal the functions of Ca2+ buffer proteins in excitable cells. *Biochimica et biophysica acta*, *1820*(8), 1294–1303. https://doi.org/10.1016/j.bbagen.2011.11.008.

Sharpley, F. C. (2009). Neurobiological pathways between chronic stress and depression: dysregulation adaptive mechanisms?. *Clinical Medicine Insights: Psychiatry, 2(), CMPsy.S3658–.* https://doi.org/10.4137/CMPsy.S3658.

Sorvari, H., Soininen, H., & Pitkänen, A. (1996). Calretinin-immunoreactive cells and fibers in the human amygdaloid complex. *The Journal of comparative neurology*, *369*(2), 188–208. https://doi.org/10.1002/(SICI)1096-9861(19960527)369:2<188::AID-CNE2>3.0.CO;2-#.

Traub, R. D., Kopell, N., Bibbig, A., Buhl, E. H., LeBeau, F. E., & Whittington, M. A. (2001). Gap junctions between interneuron dendrites can enhance synchrony of gamma oscillations in distributed networks. *The Journal of neuroscience : the official journal of the Society for Neuroscience*, *21*(23), 9478–9486. https://doi.org/10.1523/JNEUROSCI.21-23-09478.2001.

Tsai, M. J., & O'Malley, B. W. (1994). Molecular mechanisms of action of steroid/thyroid receptor superfamily members. *Annual review of biochemistry*, *63*, 451–486. https://doi.org/10.1146/annurev.bi.63.070194.002315.

Van Rossum, G., & Drake Jr, F. L. (1995). *Python reference manual*. Centrum voor Wiskunde en Informatica Amsterdam.

Vanselow, B. K., & Keller, B. U. (2000). Calcium dynamics and buffering in oculomotor neurones from mouse that are particularly resistant during amyotrophic lateral sclerosis (ALS)-related motoneurone disease. *The Journal of physiology*, *525 Pt 2*(Pt 2), 433–445. https://doi.org/10.1111/j.1469-7793.2000.t01-1-00433.x.

Wang, H. L., Sun, Y. X., Liu, X., Wang, H., Ma, Y. N., Su, Y. A., Li, J. T., & Si, T. M. (2019). Adolescent stress increases depression-like behaviors and alters the excitatory-inhibitory balance in aged mice. *Chinese medical journal*, *132*(14), 1689–1699. https://doi.org/10.1097/CM9.0000000000000313

Wickham., H. (2016). ggplot2: Elegant Graphics for Data Analysis. Springer-Verlag New York.

Wickham, H., & Bryan, J. (2019). readxl: Read Excel Files. R package version 1.3.1. https://cran.r-project.org/web/packages/readxl/index.html.

Wickham, H., Averick, M., Bryan, J., Chang, W., McGowan, L., François, R., Grolemund, G., Hayes, A., Henry, L., Hester, J., Kuhn, M., Pedersen, T.L., Miller, E., Bache, S.M., Müller, K., Ooms, J., Robinson, D., Seidel, D.P., Spinu, V.,

Takahashi, K., Vaughan, D., Wilke, C., Woo, K., & Yutani, H. (2019). Welcome to the tidyverse. Journal of Open Source Software, 4(43), 1686, https://doi.org/10.21105/joss.01686.

Wiegert, O., Pu, Z., Shor, S., Joëls, M., & Krugers, H. (2005). Glucocorticoid receptor activation selectively hampers N-methyl-D-aspartate receptor dependent hippocampal synaptic plasticity in vitro. *Neuroscience*, *135*(2), 403–411. https://doi.org/10.1016/j.neuroscience.2005.05.039.

Xiao N (2018). _ggsci: Scientific Journal and Sci-Fi Themed Color Palettes for 'ggplot2'_. R package version 2.9, https://CRAN.R-project.org/package=ggsci.

Yang, J., Han, H., Cao, J., Li, L., & Xu, L. (2006). Prenatal stress modifies hippocampal synaptic plasticity and spatial learning in young rat offspring. *Hippocampus*, *16*(5), 431–436. https://doi.org/10.1002/hipo.20181.

Yang, Y., & Calakos, N. (2013). Presynaptic long-term plasticity. *Frontiers in synaptic neuroscience*, *5*, 8. https://doi.org/10.3389/fnsyn.2013.00008.

Yuen, E. Y., Liu, W., Karatsoreos, I. N., Ren, Y., Feng, J., McEwen, B. S., & Yan, Z. (2011). Mechanisms for acute stress-induced enhancement of glutamatergic transmission and working memory. *Molecular psychiatry*, *16*(2), 156–170. https://doi.org/10.1038/mp.2010.50.

SUPPLEMENTARY INFORMATION

Fiji-ImageJ macros

We wrote six Fiji-ImageJ macros and two Python scripts for the computer-assisted image analysis. The workflow starts with the Macro 1, which creates projections out from original z-stack image piles. The projections are a sum of 5 consecutive images of the pile, which for each case are at different indexes. Macro 2 is for the manual selection of the ROIs of the brain area to be analyzed. Macro 3 provides cell soma selections and data for the calculation of quantification variables of PV and CR channels; it is the input for Python Script 2. Macro 4 measures the area of the analyzed brain ROI, discarding the space that cracks some damaged tissues have (this is necessary for the calculation of cell density). Macro 5 creates ROIs in NMDAR1 channels matching those in CR and PV (using Macro 2 output). Macro 6 calculates the information needed for colocalization analysis, and is the input for Python Script 2.

Macro 1. Creates sum projections of specified z-stacks from original TIFF images of 12 slices.

```
setBatchMode(true);

//Type the brain area and channel to process
//(and allow the corresponding zstart bellow to be read):
brain = "CA1"
channel = "ch00"

// All (38) images
input = "C:/Users/Usuario/…/"+brain+"_ordered/"+brain+"_"+channel+"/"
output = "C:/Users/Usuario/…brain+"_ordered/"+brain+"_"+channel+"_results/"

// PrL:
//zstart_ar = newArray(4,5,3,3,5,6,3,6,7,8,4,4,7,4,1,2,4,6,3,5,5,5,4,2,7,8,1,8,4,1,4,3,6,7,5,5,7,7);

// CA1:
zstart_ar = newArray(5,3,4,3,8,8,8,7,3,3,4,4,3,4,3,4,4,4,2,8,6,4,8,6,6,4,5,4,3,4,7,4,4,3,7,7);

// BLA:
//zstart_ar = newArray(4,3,5,5,3,8,5,5,4,4,3,3,5,5,5,7,3,5,8,8,8,2,3,7,4,5,6,5,5,3,3,3,3,6,3,5);

// NaC:
//zstart_ar = newArray(8,1,4,3,5,6,4,4,3,3,3,3,6,3,3,3,8,8,1,3,8,8,8,8,8,8,3,4,4,5,4,5,6,7,2,4,6,8);

// Hipo:
//zstart_ar = newArray(5,5,4,5,3,3,5,4,3,5,5,3,3,4,3,2,7,4);


list = getFileList(input);
for (i = 0; i < list.length; i++){
        open(input + list[i]);
        fname = File.getNameWithoutExtension(input + list[i]);
```

```
        ar = split(fname, "_" );
        ar1 = Array.deleteIndex(ar, 6);
                  ar2 = Array.deleteIndex(ar1, 5);
                  iname = String.join(ar2, "_");

                  zstart = zstart_ar[i];
                  zstop= zstart+4;

                  selectWindow(list[i]);
                  run("Z Project...", "start="+zstart+" stop="+zstop+" projection=[Sum Slices]");
                  print(zstart + " - " + zstop + " / " + list[i]);
                  selectWindow(list[i]);
                  close();
                  selectWindow(getTitle());
                  setOption("ScaleConversions", true);
                  run("16-bit");

                  saveAs("Tiff", output + iname + "_rawzproject.tif");
                  close();
}

selectWindow("Log");
saveAs("Text", output + ar[3] + "_z-stack.txt");
close("Log");

setBatchMode(false);
```

Macro 2. Asks the user to select a ROI (rectangle) and stores the output in a separate folder.

```
setBatchMode(true);

brain = "CA1"

input = "C:/Users/Usuario/…/"+brain+"_ordered/"+brain+"_ch02_results/"
output = "C:/Users/Usuario/…/"+brain+"_ordered/"+brain+"_rect_ROIs/"

allfiles = getFileList(input);
list = Array.filter(allfiles, "_rawzproject.tif");

for (i = 0; i < list.length; i++){
                  open(input + list[i]);
                  fname = File.getNameWithoutExtension(input + list[i]);
        ar = split(fname, "_" );
        ar1 = Array.deleteIndex(ar, 6);
        ar2 = Array.deleteIndex(ar1, 5);
                  iname = String.join(ar1, "_");
                  iname2 = String.join(ar2, "_");

                  //run("Brightness/Contrast...");
                  run("Enhance Contrast", "saturated=0.35");

        setBatchMode(false);
                  makeRectangle(1050, 588, 522, 1932);
                  roiManager("Add");
                  //setTool("rectangle");  'igual hau ez da ezta behar
                  waitForUser("Waiting for user to choose the proper ROI. Press OK to continue....");
                  setBatchMode(true);

                  roiManager("Add");
                  roiManager("Select", 1);
                  roiManager("Rename", iname2 + "_rect");
                  roiManager("Save", output + iname2 + "_rect.roi");
                  run("Select All");
                  roiManager("Deselect");
                  roiManager("Delete");
         close(getTitle());
}

run("Close");
setBatchMode(false);
```

Macro 3. Creates cell soma selections and data for quantification analysis.

```
setBatchMode(true);

Type the brain area and channel to process
brain = "CA1"
channel = "ch01"
prominence = 10000
cte = 0.55

// All images
```

```
dir = "C:/Users/Usuario/…/brain+"_ordered/"+brain+"_"+channel+"_results/"
dir_rect = "C:/Users/Usuario/…/"+brain+"_ordered/"+brain+"_rect_ROIs/"

print("brain: " +brain)
print("channel: "+channel)
print("prominence: "+prominence)
print("cte: "+cte)

saveAs("Text",  dir + "metadata.txt");
close("Log");

allfiles = getFileList(dir);
list = Array.filter(allfiles, channel+"_rawzproject.tif");

for (i = 0; i < list.length; i++){
        open(dir + list[i]);
        fname = File.getNameWithoutExtension(dir + list[i]);
        ar = split(fname, "_" );
        ar1 = Array.deleteIndex(ar, 6);
        ar2 = Array.deleteIndex(ar1, 5);
                iname = String.join(ar1, "_");
                iname2 = String.join(ar2, "_");

                selectWindow(list[i]);
                //selectWindow(getTitle());
                setOption("ScaleConversions", true);
                run("16-bit");

                open(dir_rect+iname2+"_rect.roi");
                run("Duplicate...", "title=rawzproject");
                selectWindow(list[i]);
                close(list[i]);
                selectWindow("rawzproject");
                run("Duplicate...", "title=processed");
                selectWindow("rawzproject");
                selectWindow("processed");
                run("Subtract Background...", "rolling=30");
                run("Gaussian Blur...", "sigma=2");

                run("Find Maxima...", "prominence="+prominence+" exclude output=[List]");
                for (j = 0; j < nResults(); j++) {
                x = getResult("X",j);
                         y = getResult("Y",j);
                         newcol = getPixel(x,y);
                setResult("PixelValue", j, newcol);
                         pv = getResult("PixelValue",j);
                         tolerance = pv*cte;
                         doWand(x, y, tolerance,"8-connected");
                         roiManager("add");
                         run("Select None");
                }
                updateResults();
                saveAs("Results", dir + iname + "_Results.csv");
                close("Results");
                //run("Close");
                //saveAs("Tiff", dir + iname + "_processed.tif");
                close();

                last = roiManager("Count");
                if (last != 0) {
                         roiManager("Combine");
                         roiManager("Add");
                         roiManager("Select", last);

                         run("Create Mask");

                         run("Select All");
                         roiManager("Deselect");
                         roiManager("Delete");

                         selectWindow("Mask");
                         run("Select None");
                         run("Watershed");
                         run("Analyze Particles...", "exclude add");
                         close();

                         selectWindow("rawzproject");
                         run("Set Measurements...", "area mean standard min shape integrated redirect=None
decimal=3");

                         nROIs = roiManager("Count");
                         for (k = 0; k < nROIs; k++) {
                                  roiManager("Select", k);
                                  roiManager("Rename", k+1);
                                  run("Measure");
```

```
                                        setResult("ROI_name", k, Roi.getName);
                                }

                                run("Select All");
                                if (last > 1) {
                                        roiManager("Combine");
                                }
                                run("Make Inverse");
                                run("Measure");  // measuring background
                                lastrow = Table.size()-1;
                                setResult("ROI_name", lastrow, "bg");
                                saveAs("Results", dir + iname + "_Data.csv"); // last row is background data
                                close("Results");
                        }

                        selectWindow("rawzproject");
                        if (roiManager("count") > 0) {
                                run("Select None");
                                roiManager("Show None");
                                roiManager("Deselect");
                                roiManager("Save", dir + iname + "_ROIs.zip");
                                roiManager("Delete");
                                close("Manager");
                        }
                        saveAs("Tiff", dir + iname + "_rect_rawzproject.tif");
                        close();
}

setBatchMode(false);
```

Macro 4. Creates the total CA1 area without cracks ROIs and measures the area (it uses ch01 images, but the resulted ROI can be used over any channel).

```
setBatchMode(true);

//Type the brain area and channel to process
brain = "CA1"

// All images
input = "C:/Users/Usuario/…/"+brain+"_ordered/"+brain+"_ch01_results/"
input_rect = "C:/Users/Usuario/…/"+brain+"_ordered/"+brain+"_rect_ROIs/"
output = "C:/Users/Usuario/…/"+brain+"_noCracks/"

allfiles = getFileList(input);
list = Array.filter(allfiles, "rect_rawzproject.tif");
rectfiles = getFileList(input_rect);

for (i = 0; i < list.length; i++){
        open(input + list[i]);
        fname = File.getNameWithoutExtension(input + list[i]);
        ar = split(fname, "_" );
        ar1 = Array.deleteIndex(ar, 6);
        ar2 = Array.deleteIndex(ar1, 5);
        iname = String.join(ar2, "_");

                open(input_rect+rectfiles[i]);
                run("Crop");

                selectWindow(list[i]);
                run("Gaussian Blur...", "sigma=0.5");
                setAutoThreshold("Default dark");
                //run("Threshold...");
                setThreshold(0.0000, 0.0000);
                setOption("BlackBackground", false);
                run("Convert to Mask");
                run("Dilate");
                run("Fill Holes");
                run("Analyze Particles...", "size=1000.00-Infinity add");

                run("Set  Measurements...",  "area  mean  standard  min  shape  integrated  redirect=None
decimal=3");

                nROIs = roiManager("Count");
                if (nROIs != 0) {
                        run("Select All");
                        roiManager("Combine");
                        run("Make Inverse");
                        roiManager("add");
                } else {
                        run("Select All");
                        roiManager("add");
                }
                roiManager("Select", roiManager("Count")-1);
```

```
                    roiManager("Rename", "Area_"+iname);
                    run("Measure");  // measuring ROI_Area
                    roiManager("Select", roiManager("Count")-1);
                    //roiManager("Select", newArray(roiManager("Count")-2));
                    //roiManager("Delete");
                    roiManager("Save", output + iname + "_noCracksROI.roi");
                    run("Select All");
                    roiManager("Deselect");
                    roiManager("Delete");

                    setResult("name", i, iname);

                    selectWindow(list[i]);
                    close();
                    run("Close");
}

saveAs("Results", output + brain + "_noCracksArea.csv")
close("Results");

setBatchMode(false);
```

Macro 5. Creates rect_rawzprojects of ch00 for the colocalization study.

```
setBatchMode(true);

brain = "CA1"

dir = "C:/Users/Usuario/…/"+brain+"_ordered/"+brain+"_ch00_results/"
dir_rect = "C:/Users/Usuario/…/"+brain+"_ordered/"+brain+"_rect_ROIs/"

allfiles = getFileList(dir);
list = Array.filter(allfiles, "ch00_rawzproject.tif");

for (i = 0; i < list.length; i++){
        open(dir + list[i]);
        fname = File.getNameWithoutExtension(dir + list[i]);
        ar = split(fname, "_" );
        ar1 = Array.deleteIndex(ar, 6);
        ar2 = Array.deleteIndex(ar1, 5);
        iname2 = String.join(ar2, "_");

                    open(dir_rect+iname2+"_rect.roi");
                    run("Crop");
                    //selectWindow(list[i]);
                    saveAs("Tiff", dir + iname2 + "_ch00_rect_rawzproject.tif");
                    close();
}

setBatchMode(false);
```

Macro 6. Returns filtered ROIs set and colocalization information corresponding to the ch00.

```
setBatchMode(true);

//Type the brain area and channel to process
brain = "CA1"
channel = "ch01"
zproject = "rect_rawzproject" // specify if it is "rect_rawzproject" or "rawzproject".

// All images
dir00 = "C:/Users/Usuario/…/"+brain+"_ordered/"+brain+"_ch00_results/"
dir0X = "C:/Users/Usuario/…/"+brain+"_ordered/"+brain+"_"+channel+"_results/"

function findRoiWithName(roiName) {
         nR = roiManager("Count");

         for (i=0; i<nR; i++) {
                    roiManager("Select", i);
                    rName = Roi.getName();
                    if (matches(rName, roiName)) {
                              return i;
                    }
         }
         return 1;
}


run("Set Measurements...", "area mean standard min integrated redirect=None decimal=3");

filesdir00 = getFileList(dir00);
list = Array.filter(filesdir00, "ch00_"+zproject+".tif");
filesdir0X = getFileList(dir0X);
```

```
ROIsfiles = Array.filter(filesdir0X, channel+"_ROIs.zip");

for (j = 0; j < ROIsfiles.length; j++){
    fname = File.getNameWithoutExtension(dir00 + ROIsfiles[j]);
    ar = split(fname, "_" );
    ar1 = Array.deleteIndex(ar, 6);
    ar2 = Array.deleteIndex(ar1, 5);
    //ar3 = Array.deleteIndex(ar2, 5);
         iname = String.join(ar1, "_");
         iname2 = String.join(ar2, "_");
         for (i = 0; i < list.length; i++) {
                  if (list[i].startsWith(iname2)) {
                           open(dir00 + list[i]);
         open(dir0X+"coloc_"+brain+"_"+channel+".csv");
                           Table.rename("coloc_"+brain+"_"+channel+".csv", "Results");
                           headings = split(String.getResultsHeadings);

                           roiManager("Open", dir0X+iname2+"_"+channel+"_ROIs.zip");

                           ROIseq = newArray;
                           head = headings[i];

                           for (k = 0; k < nResults(); k++) {
                                    v = getResult(head, k);
                           ROIseq = Array.concat(ROIseq, v);
                           }

                           ROIseq2 = newArray;
                           for (n = 0; n < lengthOf(ROIseq); n++) {
                                    if (isNaN(ROIseq[n])) {
                                             continue;
                                    } else {
                                             ROIseq2 = Array.concat(ROIseq2, ROIseq[n]);
                                    }
                           }

                           for (m = 0; m < lengthOf(ROIseq2); m++) {
                                    roiManager("Select", findRoiWithName(ROIseq2[m]+1));
                                    roiManager("Delete");
                           }

                           if (roiManager("count") > 0) {
                                    roiManager("Save", dir0X+iname2+"_"+channel+"_filteredROIs.zip");

                                    close("Results");

                                    nROIs = roiManager("Count");
                                    for (l = 0; l < nROIs; l++) {
                                             roiManager("Select", l);
                                             run("Measure");
                                             setResult("ROI_name", l, Roi.getName);
                                    }

                                    run("Select All");
                                    roiManager("Deselect");
                                    roiManager("Delete");
                           } else {
                                    close("Results");
                           }

                           selectWindow(list[i]);
                           run("Duplicate...", "title=mask.tif");
                           selectWindow("mask.tif");

                           setAutoThreshold("Triangle dark");
                           //run("Threshold...");
                           setOption("BlackBackground", false);
                           run("Convert to Mask");
                           run("Analyze Particles...", "size=20-Infinity add");
                           close("mask.tif");

                           last = roiManager("count");
                           if (last != 0) {
                                    if (last > 1) {
                                             run("Select All");
                                             roiManager("Combine");
                                    }
                                    run("Make Inverse");
                                    run("Measure");  // measuring background
                           } else {
                                    run("Select None");
                                    run("Measure");
                           }
                           selectWindow("Results");
                           lastrow = Table.size()-1;
```

```
                            setResult("ROI_name", lastrow, "bg");
                            saveAs("Results", dir0X + iname + "_ColocData.csv"); // last row is background
data
                            close("Results");

                            if (roiManager("count") != 0) {
                                     run("Select All");
                                     roiManager("Deselect");
                                     roiManager("Delete");
                            }
                            close("Manager");

                            selectWindow(list[i]);
                            close();
                    }
            }
}

setBatchMode(false);
```

Python scripts

Script 1 works on Fiji-ImageJ Macro 3 data output and provides information of the variables of the quantification study for the subsequent statistical analysis. Script 2 analyzes Macro 6 data output and returns variables of the colocalization study for the subsequent statistical analysis.

Script 1. Creates output of quantification variables and provides filtering information for Macro 4.

```
# %% Libraires

import os
import pandas as pd #for dataframe handling
pd.set_option('display.max_rows', None)
pd.set_option('display.max_columns', None)
pd.set_option('display.width', None)
pd.set_option('display.max_colwidth', None)
import numpy as np #for statistics
from xlwt import Workbook


# %% Defining functions

def CTCF(i, df_filt, df1, df2):  # i = index of row of a dataframe, df = a dataframe
    '''calculates the CTCF for each cell-ROI'''
    IDvalue = df_filt.at[i,'IntDen']
    Avalue = df_filt.at[i,'Area']
    bg1 = df1.loc[df1.index[-1], "Mean"]
    bg2 = df2.loc[df2.index[-1], "Mean"]
    BGvalue = (bg1+bg2)/2 # from the last row (background)
    CTCF = (IDvalue - (Avalue * BGvalue))
    return CTCF

def mean_sd(lst):
    '''just mean and sd of the CTCF set of cell-ROIs of an image (*Data.csv)'''
    Mean = np.mean(lst)
    SD = np.std(lst)
    return (Mean, SD)


# %% Loading data

# Type the brain area and channel to analyze:
brain = 'CA1'
channel = 'ch02'

stemdir = 'C:/Users/Usuario/…/'
src = stemdir + brain + '_ordered/' + brain + '_' + channel + '_results/'

filelist = []
files = os.listdir(src)
for i in files:
   if i.endswith('_Data.csv'):
       filelist.append(i)

src2 = stemdir + 'totalAreaWithNoCracks/' + brain + '_noCracks/'
df_tA = pd.read_csv(src2 + brain + '_noCracksArea.csv')

dst = 'C:/Users/Usuario/Desktop/'
```

```
# New data: cellN and CTCF (mean_sd)

hem_list = []

for i in filelist:
    fullpath = src + '/' + i # el '/' está de sobra, verdad?????
    hem = pd.read_csv(fullpath)
    hem.rename(columns={'Circ.':'Circ',
                        ' ':'ROI_index'},
               inplace=True)
    arg1 = hem
    hem_list.append(arg1)

df_list = []
cellN = []
df_filt_list = []
dfC_list = []

for i in range(0, len(filelist), 2):
    hem1 = hem_list[i][:-1]
    hem2 = hem_list[i+1][:-1]
    dfC1 = hem_list[i]
    dfC2 = hem_list[i+1]
    arg = (dfC1, dfC2)
    dfC_list.append(arg)

    frames = [hem1, hem2]
    df = pd.concat(frames)
    df = df.reset_index()
    df_list.append(df)

    #df_filt = df[(df['Area'] > 60) & (df['Area'] < 1000) & (df['Circ'] > 0.55)] # the best for ch01
    #df_filt = df[(df['Area'] > 75) & (df['Area'] < 1000) & (df['Circ'] > 0.65)] # the best for ch02
    df_filt = df[(df['Area'] > 75) & (df['Area'] < 1000) & (df['Circ'] > 0.55)] # the best for CA1_ch02

    df_filt = df_filt.reset_index()
    df_filt_list.append(df_filt)

    cN = len(df_filt)
    cellN.append(cN)

CTCF_list_list = []

for i in range(len(cellN)):
    CTCF_list    =    [CTCF(j,    df_filt_list[i],    dfC_list[i][0],    dfC_list[i][1])    for    j    in
range(len(df_filt_list[i]))]
    CTCF_list_list.append(CTCF_list)
    CTCF_stat = [mean_sd(k) for k in CTCF_list_list]


# Preparing the data

nm_list = []
for i in range(0, len(filelist), 2):
    sel_nm = [filelist[i].split('_')[index] for index in [0,1,2,3]]
    nm_list.append(sel_nm)
image_name = ['_'.join(nm) for nm in nm_list]

tA_hem_list = df_tA.loc[:, ['name','Area']].values.tolist()
tArea = [tA_hem_list[i][1]+tA_hem_list[i+1][1] for i in range(0, len(tA_hem_list), 2)]

CTCF_mean, CTCF_sd = map(list, zip(*CTCF_stat))

cellD = [cellN[i]/((tArea[i]*7.6)*10**(-9)) for i in range(len(cellN))]

image_name.insert(0, 'image_name')
cellD.insert(0, channel)
CTCF_mean.insert(0, 'CTCF_mean_'+channel)
CTCF_sd.insert(0, 'CTCF_sd_'+channel)


#  Create the workbook for cell quantification + CTCF

workbook = Workbook()
wsheet = workbook.add_sheet('Sheet')

for row_num, data in enumerate(image_name):
        wsheet.write(row_num, 0, data)

for row_num, data in enumerate(cellD):
       wsheet.write(row_num, 1, data)

for row_num, data in enumerate(CTCF_mean):
       wsheet.write(row_num, 2, data)
```

```
for row_num, data in enumerate(CTCF_sd):
       wsheet.write(row_num, 3, data)


workbook.save(dst+'qt_stress/byanimal_'+brain+'_'+channel+'.xls') #
```

Script 2. Creates output of colocalization variables.

```
# %% Libraires

import os
import pandas as pd #for dataframe handling
pd.set_option('display.max_rows', None)
pd.set_option('display.max_columns', None)
pd.set_option('display.width', None)
pd.set_option('display.max_colwidth', None)
import numpy as np #for statistics
from xlwt import Workbook


# %% Defining functions

def CTCF(i, df_filt, df1, df2):  # i = index of row of a dataframe, df = a dataframe
    '''calculates the CTCF for each cell-ROI'''
    IDvalue = df_filt.at[i,'IntDen']
    Avalue = df_filt.at[i,'Area']
    bg1 = df1.loc[df1.index[-1], "Mean"]
    bg2 = df2.loc[df2.index[-1], "Mean"]
    BGvalue = (bg1+bg2)/2 # from the last row (background)
    CTCF = (IDvalue - (Avalue * BGvalue))
    return CTCF

def mean_sd(lst):
    '''just mean and sd of the CTCF set of cell-ROIs of an image (*Data.csv)'''
    Mean = np.mean(lst)
    SD = np.std(lst)
    return (Mean, SD)

def percentage(i, lst_pos, lst_total):
    positive = len(lst_pos[i][1])
    total = len(lst_total[i][1])
    if not total == 0:
        per = (positive/total) * 100
    else:
        per = float("NaN")
    return per


# %% Loading data

# Type the brain area and channel to analyze:
brain = 'BLA'
channel = 'ch02'

stemdir = 'C:/Users/Usuario/…/'
src = stemdir + brain + '_ordered/' + brain + '_' + channel + '_results/'

filelistch00 = []
filelistch0X = []
files = os.listdir(src)
for i in files:
   if i.endswith('_Data.csv'):
       filelistch0X.append(i)
   if i.endswith('_ColocData.csv'):
       filelistch00.append(i)

src2 = stemdir + 'totalAreaWithNoCracks/' + brain + '_noCracks/'
df_tA = pd.read_csv(src2 + brain + '_noCracksArea.csv')

dst = 'C:/Users/Usuario/Desktop/'

nm_list = []
for i in range(0, len(filelistch00), 2):
    sel_nm = [filelistch00[i].split('_')[index] for index in [0,1,2,3]]
    nm_list.append(sel_nm)
image_name = ['_'.join(nm) for nm in nm_list]


#  New data: CTCF of ch00 (CTCF_list_list0) and CTCF_stat0 (mean and sd of ch00, del total de células)

hemX_list = []
```

```
for i in filelistch0X:
    fullpath = src + '/' + i # el '/' está de sobra, verdad?????
    hemX = pd.read_csv(fullpath)
    hemX.rename(columns={'Circ.':'Circ',
                         ' ':'ROI_index'},
              inplace=True)
    arg1 = hemX
    hemX_list.append(arg1)

dfX_list = []
cellN = []
dfX_filt_list = []
dfCX_list = []

for i in range(0, len(filelistch0X), 2):
    hem1 = hemX_list[i][:-1]
    hem2 = hemX_list[i+1][:-1]
    dfC1 = hemX_list[i]
    dfC2 = hemX_list[i+1]
    arg = (dfC1, dfC2)
    dfCX_list.append(arg)

    frames = [hem1, hem2]
    df = pd.concat(frames)
    df = df.reset_index()
    dfX_list.append(df)

    #dfX_filt = df[(df['Area'] > 60) & (df['Area'] < 1000) & (df['Circ'] > 0.55)] # the best for ch01
    dfX_filt = df[(df['Area'] > 75) & (df['Area'] < 1000) & (df['Circ'] > 0.65)] # the best for ch02

    dfX_filt = dfX_filt.reset_index()
    dfX_filt_list.append(dfX_filt)

    cN = len(dfX_filt)
    cellN.append(cN)

CTCF_list_listX = []
CTCF_list_listX_withROI = []

for i in range(len(cellN)):
    CTCF_listX    =    [CTCF(j,    dfX_filt_list[i],    dfCX_list[i][0],    dfCX_list[i][1])    for    j    in
range(len(dfX_filt_list[i]))]
    CTCF_list_listX.append(CTCF_listX)
    CTCF_statX = [mean_sd(k) for k in CTCF_list_listX]
    CTCF_listX_ROI = [*zip(dfX_filt.ROI_name.values.tolist(), CTCF_listX)] #el ROI_name de ch00 es igual que
el ROI_index de filtered ch0X
    arg2 = (image_name[i], CTCF_listX_ROI)
    CTCF_list_listX_withROI.append(arg2)


# New data: CTCF of ch00 (CTCF_list_list0) and CTCF_stat0 (mean and sd of ch00, del total de células)

hem0_list = []

for i in filelistch00:
    fullpath = src + '/' + i # el '/' está de sobra, verdad?????
    hem0 = pd.read_csv(fullpath)
    hem0.rename(columns={' ':'ROI_index'},
              inplace=True)
    arg1 = hem0
    hem0_list.append(arg1)

df0_list = []
cellN = []
df0_filt_list = []
dfC0_list = []

for i in range(0, len(filelistch00), 2):
    hem1 = hem0_list[i][:-1]
    hem2 = hem0_list[i+1][:-1]
    dfC1 = hem0_list[i]
    dfC2 = hem0_list[i+1]
    arg = (dfC1, dfC2)
    dfC0_list.append(arg)

    frames = [hem1, hem2]
    df = pd.concat(frames)
    df = df.reset_index()
    df0_filt_list.append(df) # it is "already filtered", meanung that we just analyzed those rois after
filtering in ch0X.

    cN = len(df)
    cellN.append(cN)

CTCF_list_list0 = []
```

```
CTCF_list_list0_withROI = []

for i in range(len(cellN)):
    CTCF_list0    =    [CTCF(j,    df0_filt_list[i],    dfC0_list[i][0],    dfC0_list[i][1])    for    j    in
range(len(df0_filt_list[i]))]
    CTCF_list_list0.append(CTCF_list0)
    CTCF_stat0 = [mean_sd(k) for k in CTCF_list_list0]
    CTCF_list0_ROI = [*zip(df0_filt_list[i].ROI_name.values.tolist(), CTCF_list0)] #el ROI_name de ch00 es
igual que el ROI_index de filtered ch0X
    arg2 = (image_name[i], CTCF_list0_ROI)
    CTCF_list_list0_withROI.append(arg2)


# New data: percentages (ch00-positive cells over total ch0X-postive cells)

# First, create a list with ch00 filtered lists:
CTCF_lists_filtered = []
for i, name in enumerate(CTCF_list_list0_withROI):
    new_list = []
    for index, item in enumerate(CTCF_list_list0_withROI[i][1]):
        if item[1] > 50000: # decidir qué filtro!
            new_list.append(item)
    arg = (name[0], new_list)
    CTCF_lists_filtered.append(arg)

# Calculate percentages:
percentages    =    [percentage(i,    CTCF_lists_filtered,    CTCF_list_list0_withROI)    for    i    in
range(len(CTCF_list_list0_withROI))]

# PC
PC_list = []

for i in range(len(CTCF_list_list0)):
    var_ch00 = np.array(CTCF_list_list0[i])
    var_ch0X = np.array(CTCF_list_listX[i])
    my_rho = np.corrcoef(var_ch00, var_ch0X)
    PC_list.append(my_rho[0][1])


# Preparing the data

CTCF_mean0, CTCF_sd0 = map(list, zip(*CTCF_stat0))

image_name.insert(0, 'image_name')
percentages.insert(0, 'pct_'+channel)
CTCF_mean0.insert(0, 'CTCF_mean_ch00_'+channel)
CTCF_sd0.insert(0, 'CTCF_sd_ch00_'+channel)
PC_list.insert(0, 'PC_'+channel)


# Create the workbook for cell quantification + CTCF

workbook = Workbook()
wsheet = workbook.add_sheet('Sheet')

for row_num, data in enumerate(image_name):
        wsheet.write(row_num, 0, data)

for row_num, data in enumerate(percentages):
        wsheet.write(row_num, 1, data)

for row_num, data in enumerate(CTCF_mean0):
       wsheet.write(row_num, 2, data)

for row_num, data in enumerate(CTCF_sd0):
       wsheet.write(row_num, 3, data)

for row_num, data in enumerate(PC_list):
       wsheet.write(row_num, 4, data)

workbook.save(dst+'info_coloc/byanimal_info_coloc_'+brain+'_'+channel+'.xls')
```